JOURNAL OF MAGNETIC RESONANCE **127,** 65–72 (1997)
ARTICLE NO. MN971177

Dynamic T_1 Measurement Using Snapshot-FLASH MRI

A. Jivan, M. A. Horsfield,* A. R. Moody,† and G. R. Cherryman

*Department of Radiology and *Department of Medical Physics, University of Leicester, Leicester Royal Infirmary, Leicester LE1 5WW, United Kingdom*

Received June 13, 1996; revised April 10, 1997

The application of an inversion-recovery snapshot FLASH (*f*ast *l*ow-*a*ngled *sh*ot) imaging sequence to the dynamic measurement of monoexponential T_1 relaxation was investigated. The effect of (a) a reduction in the overall sequence repetition time, and (b) an increase of the read-pulse flip angle, on the measurement of T_1 was analyzed. The error in T_1 introduced by these factors is calculated, and a fuller analysis that takes them into account is presented. Data from a phantom are used to confirm this analysis. The magnitude of the errors is illustrated by measuring myocardial T_1 in patients with acute ischaemic heart disease during the injection of a bolus of the contrast medium gadobenate dimeglumine. Overall, there was a 10% difference between the T_1 values when the approximate and exact solutions were used; this was statistically significant. However, the difference was on average 25% for patients with a high heart rate (because of the shorter sequence-repetition time) in areas of infarcted myocardium (because of the longer T_1).

INTRODUCTION

T_1 and T_2 are intrinsic tissue parameters that are altered in some pathological tissues (*1*). It was hoped that accurate measurement of these parameters would distinguish between normal and pathological tissue. However, the wide biological heterogeneity of relaxation times (*2*) makes them poor diagnostic indicators. This may at least partly be attributable to the inaccuracy of the experimental methods used in the clinical scanning situation (*3, 4*).

A one-shot sequence that allows precise T_1 measurements is TOMROP (*T o*ne by *m*ultiple *r*ead-*o*ut *p*ulses) (*5*) first proposed for spectroscopy by Look and Locker (*6*) and adapted for imaging by Graumann *et al.* (*7*). This was denoted one-shot, as it requires only one imaging experiment to acquire a series of images for T_1 calculation. In this sequence, the longitudinal magnetization is repeatedly sampled (1 sample per image) as it approaches a steady state, either from an unperturbed state or following a 90° or 180° pulse. This is repeated for each phase-encoding step, to produce a series of images with different T_1 weightings, and requires approximately 10 minutes of imaging time. Variants of this (*8–11*) have been used to measure multiexponential relaxation (*9, 10, 12*) required for accurate evaluation of T_1 in some tissues.

Multiple images have been obtained with an inversion-recovery snapshot-FLASH (*f*ast *l*ow-*a*ngled *sh*ot) or TurboFLASH imaging sequence (*13*), and used to measure T_1. Here an inversion pulse is applied, and as the longitudinal magnetization recovers, a series of images is acquired. Each image is formed by applying a train of low-flip-angle pulses, each of which gives one phase-encode line. There is a change in longitudinal magnetization due to the application of the readout pulses, and a method of correction for this has been shown (*14*).

If T_1 is changing rapidly, then methods that need multiple images may not be practical. Measurement of T_1 can be achieved in the shortest time by repeatedly acquiring just a single T_1-weighted image, which, in conjunction with a static measure of the equilibrium magnetization, can be used to calculate T_1. In this context, we have investigated the inversion-recovery snapshot-FLASH sequence (*13*), for dynamically measuring T_1, assuming monoexponential relaxation (*15*). Here, an inversion pulse is applied, and after the inversion time (TI), a train of readout pulses gives a single image in one shot. The contrast in the image is determined by the position of the central phase-encoding step in the longitudinal relaxation curve, and can be altered by changing TI.

In this study, we look at the effects of the flip angle of the readout pulses and the repetition rate of the scans on the accuracy of measuring T_1. We then show the magnitude of the errors which would be expected when measuring *in vivo* myocardial T_1 during the injection of a bolus of contrast medium for perfusion assessment if these confounding factors were not taken into account.

THEORY

We consider here what happens to the measured signal intensity in a snapshot-FLASH sequence when the overall sequence repetition time cannot be considered long with

† Present address: Department of Academic Radiology, University of Nottingham, Queens Medical Centre, Nottingham NG7 2UH, United Kingdom.

1090-7807/97 $25.00

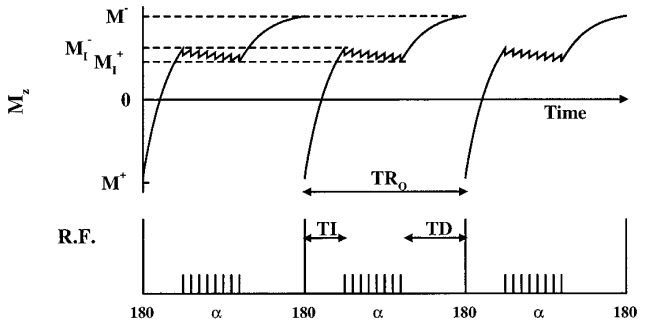

FIG. 1. Schematic representation of the z magnetization during the snapshot-FLASH sequence in steady state. TR_0 is the image repetition time; TI is the inversion time; and TD is the post-image recovery/trigger delay. The longitudinal magnetization values are marked just before the inversion pulse (M^-); just after the inversion pulse (M^+); just before the start of image acquisition (M_I^-); and at the end of image acquisition (M_I^+).

respect to T_1. Normally, the start of the sequence in dynamic cardiac studies is triggered from the ECG, and therefore TR_0 will be an integer multiple of the R-wave interval. For simplicity, a single-slice experiment is analyzed.

The T_1-weighted snapshot-FLASH sequence (illustrated schematically in Fig. 1) can be written

$$[\mathrm{TD}—180°—\mathrm{TI}—[\alpha—\mathrm{TR}]_{Nk}]_{Ni}, \qquad [1]$$

where TD is an optional delay before the start of the sequence; TI is the inversion time; and α is the flip angle of the read pulse for acquisition of one line of k space. The inner loop is repeated for Nk lines of k space, and the outer loop is repeated Ni times, according to the number of images required. When more than one image is acquired, the signal intensity is affected by the pulses from the previous image, and analysis becomes more complicated. Also, the α pulses cause increasing saturation through the sequence, and therefore, for simplicity, we assume that the signal intensity seen in the final image reflects the intensity of the mid-line of k space, from which most of the image contrast is derived. Rostrup *et al.* (*16*) recently showed the effect of the α pulses on measured signal intensity. We now extend their results to show the correction needed when the overall sequence repetition time does not allow complete relaxation.

Using the notation in Fig. 1, we can write expressions for the z magnetization at four stages in the snapshot-FLASH sequence. After several sequence repetitions, when a steady state is reached, the magnetization at the end of the TD delay is of equal magnitude, but of opposite sign, to that just after the previous 180° pulse. Thus,

$$M^+ = -M^-. \qquad [2]$$

Longitudinal relaxation then occurs during the TI period such that the magnetization just before the first α pulse for image acquisition is

$$M_I^- = M_0(1 - \mathrm{EI}) + M^+\mathrm{EI}, \qquad [3]$$

where $\mathrm{EI} = \exp(-\mathrm{TI}/T_1)$, and M_0 is the equilibrium z magnetization. After the final α pulse, the effect of the sequence of α pulses (*16*) is such that

$$M_I^+ = M_I^-(\mathrm{ER}\cos(\alpha))^{Nk} + M_0(1 - \mathrm{ER})\left\{\frac{[\mathrm{ER}\cos(\alpha)]^{Nk} - 1}{\mathrm{ER}\cos(\alpha) - 1}\right\}, \qquad [4]$$

where $\mathrm{ER} = \exp(-\mathrm{TR}/T_1)$. At the end of image acquisition, relaxation occurs during the period TD before the next inversion pulse. So, just before the inversion pulse

$$M^- = M_0(1 - \mathrm{ED}) + M_I^+\mathrm{ED}, \qquad [5]$$

where $\mathrm{ED} = \exp(-\mathrm{TD}/T_1)$. Solution of this system of equations leads to a z magnetization value just before the mth line of k space of

$$\frac{M_m}{M_0} = C^{(m-1)}\left\{1 - \mathrm{EI}\left\{1 + \frac{\left[1 - \mathrm{ED}(1 - C^{Nk}(1 - \mathrm{EI})) + \dfrac{\mathrm{ED}(\mathrm{ER} - 1)(C^{Nk} - 1)}{C - 1}\right]}{1 + \mathrm{ED} \times C^{Nk} \times \mathrm{EI}}\right\}\right\} + (1 - \mathrm{ER})\left(\frac{C^{(m-1)} - 1}{C - 1}\right) \qquad [6]$$

where $C = \mathrm{ER}\cos(\alpha)$. The signal intensity measured is thus $M_m\sin(\alpha)$.

Equation [6] can be considerably simplified if a low flip angle is used for the α pulses. The time from the inversion pulse to the mid-line of k space is usually called the *effective* TI (TI*eff*) and is often $\mathrm{TI} + [\mathrm{TR} \times (N_k/2 - 1)]$. Also, the overall image-repetition time is $\mathrm{TR}_0 = \mathrm{TI} + (N_k \times \mathrm{TR}) + \mathrm{TD}$.

For very-low-flip-angle α pulses, Eq. [6] then reduces to

$$M = M_0\left[1 - \frac{2\exp(-\mathrm{TI}_{\mathrm{eff}}/T_1)}{(1 + \exp(-\mathrm{TR}_0/T_1))}\right], \qquad [7]$$

where M_0 is now the signal intensity that would be observed with a very long inversion time. When the TR_0 is large compared to T_1, this further reduces to

$$M = M_0[1 - 2\exp(-\mathrm{TI}_{\mathrm{eff}}/T_1)], \qquad [8]$$

which has been used in previous studies of dynamic contrast uptake (*17*). Using this expression, it is then a simple matter to calculate the T_1

$$T_1(t) = -\frac{\mathrm{TI}_{\mathrm{eff}}}{\ln\left[\frac{1}{2}\left(1 - \frac{M(t)}{M_0}\right)\right]}. \qquad [9]$$

However, when the TR_0 cannot be considered large with respect to T_1, Eq. [7] must apply, from which we have been unable to extract an analytic solution for T_1. Iterative methods must be applied in order to find the T_1 from a signal intensity ratio $[M(t)/M_0]$, even for the low-flip-angle approximation.

From Eq. [7], the null point is given by

$$\mathrm{TI}_{\mathrm{eff}} = -\ln\left[\frac{1}{2}\left(1 + \exp\left(-\frac{\mathrm{TR}_0}{T_1}\right)\right)\right]T_1. \qquad [10]$$

Often, in order to maximize the signal dynamic range in contrast-enhanced studies, the tissue to be evaluated is initially nulled before a contrast agent is introduced. In the short TR_0 regime, this then leads to a signal intensity relationship of

$$\frac{M(t)}{M_0} = 1 - \frac{2\exp\left\{\ln\left[\frac{1}{2}\left(1 + \exp\left(\frac{\mathrm{TR}_0}{T_1\mathrm{pre}}\right)\right)\right]\frac{T_1\mathrm{pre}}{T_1(t)}\right\}}{1 + \exp(-\mathrm{TR}_0/T_1(t))}, \qquad [11]$$

where T_1pre is the precontrast longitudinal relaxation time of the tissue, and $T_1(t)$ is the relaxation time measured during this dynamic experiment. Figure 2 shows a plot of this function for typical values of T_1 and TR_0. T_1pre is 750 ms, typical of myocardium. The TR_0 varies between 0.5 and 5 times T_1pre (between 0.375 and >3.75 s). The effective inversion time to achieve nulling precontrast then varies accordingly between 165 and 519 ms. As can be seen, considerable differences in the shape of signal intensity response occur as TR_0 is shortened, and it would only be possible to evaluate T_1 by taking into account both the inversion time and the overall sequence repetition time. As TR_0 is shortened, the response becomes flatter around the null point, with steeper response at lower T_1 values.

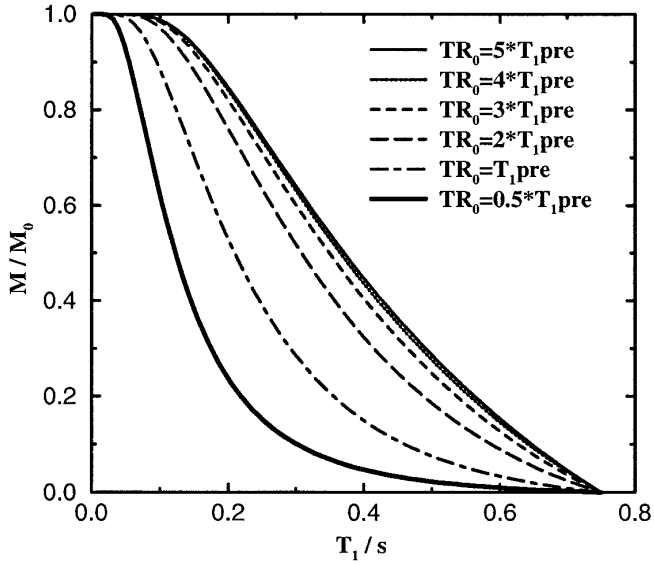

FIG. 2. Signal intensity as a function of T_1 for various overall repetition times. The values are normalized to an image without the inversion pulse and with a long repetition time. A low flip angle for the α pulses is assumed in these plots.

Low-flip-angle α pulses may not be practical in a clinical imaging situation where the signal-to-noise ratio must also be considered. We now examine the behavior of Eq. [6] for increasing flip angles and the following sequence parameters: 64 lines of *k* space with the mid-line being line 32; TR = 4.7 ms; T_1pre = 750 ms; $\mathrm{TR}_0 = T_1$pre. Figure 3 shows the effect of increasing flip angle on image signal-intensity ratio across the range of T_1 values. The approximation of low-flip-angle α pulses will clearly lead to errors in T_1 estimation for moderate flip angles. The full equation, Eq. [6], should be used when flip angles exceed a few degrees. However, this leads to the further complication that the signal intensity measured even with full relaxation before the image acquisition now depends not only on the proton density, but also on the T_1 of the tissue. Thus, the M_0 value in Eq. [6] cannot be found strictly from a single scan without an inversion pulse. Figure 4 shows the variation in signal amplitude (normalized to the value for very short T_1) that would

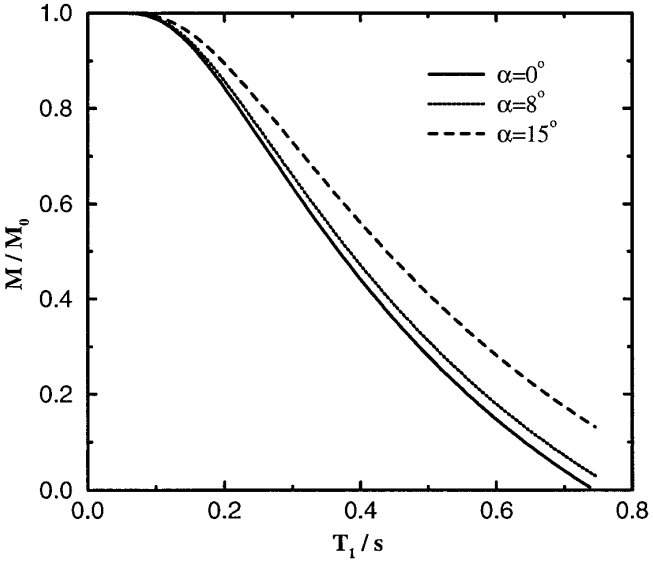

FIG. 3. The simulated effect of increasing flip angle on the image signal-intensity ratio, for a range of T_1 values at $TR_0 > 5 \times T_1$pre.

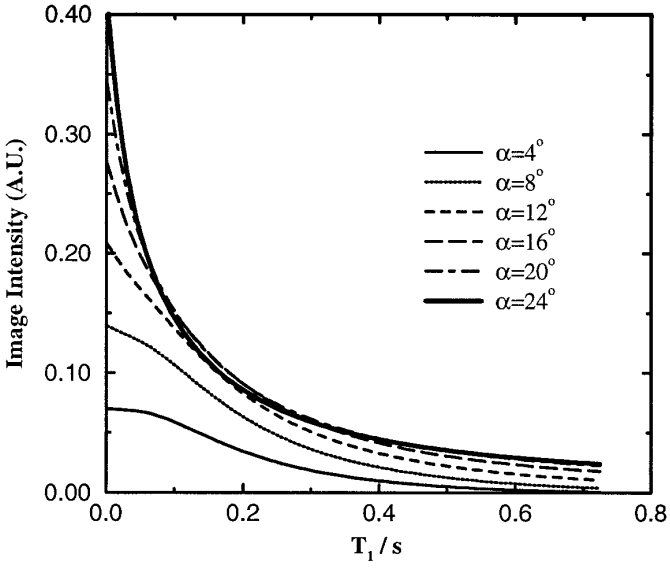

FIG. 5. The simulated effect of flip-angle increase on signal amplitude for a range of T_1 values. For T_1 values above 0.1 s, no improvement in image intensity is seen if the flip angle is increased above 12°, for the set of sequence parameters described in the text.

be seen in the ''M_0'' image, for increasing flip angles, and across the range of T_1 values, again for the example sequence parameters above. For flip angles up to about 8°, the change in signal amplitude in the M_0 image is relatively small across a quite large range of T_1 values. Thus, if we know the approximate tissue T_1 at the time when the M_0 image is acquired, we can compute a correction factor for the M_0 value in subsequent dynamic measurement using Eq. [6].

In order to choose the best flip angle, the measured signal amplitude over the range of T_1 values must be assessed. Figure 5 shows the measured signal amplitude over a range of flip angles for the same sequence parameters as above. For the lowest T_1 values, the signal amplitude continues to increase as the flip angle increases up to 90°. However, over the whole range of T_1 values, flip angles above 12° do not increase the signal amplitude greatly in this example. Although not taken into account in Fig. 5, the inversion time needs to be reduced still further if the same T_1 is to be nulled.

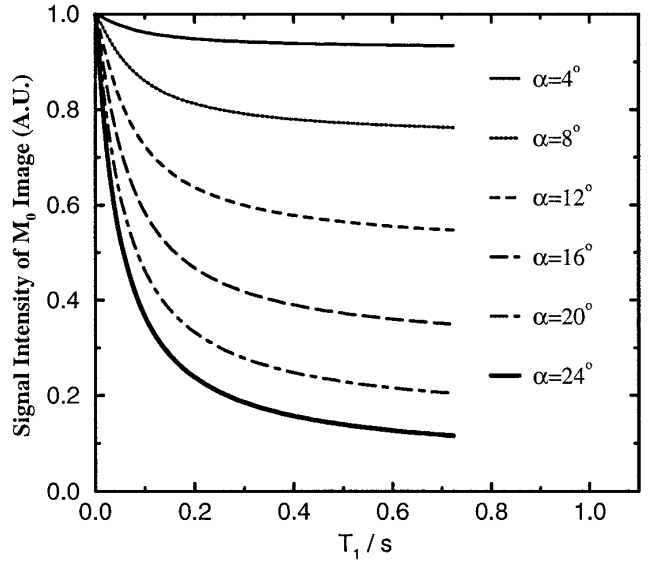

FIG. 4. The simulated effect of flip-angle increase on the signal intensity of an ''M_0'' image for a range of T_1 values.

METHODS

All experiments were performed using a whole-body MRI system (MAGNETOM, Siemens, Erlangen, Germany) operating at 1.0 T. A linearly polarized body coil was used for RF transmission and reception of the NMR signal. The system was equipped with actively shielded magnetic field gradient coils, giving gradient strengths of up to 15 mT m^{-1} with rise times of 1 ms.

A phantom consisting of seven separate vials each containing water doped with a different concentration (0.238 to 1.608 mmol/L) of Gd-DTPA (Omniscan, Nycomed, Norway) was used to give a range of T_1 values. The T_1 values of these solutions were estimated using a saturation-recovery gradient-echo sequence with TR values decreasing from 4300 to 41 ms, in 19 steps. The field of view (FOV) was 300 mm, 1 slice of 10 mm thickness was acquired with a 256×256 data matrix, and the echo time (TE) was 10 ms. Nonlinear curve fitting to a plot of signal intensity against TR was performed using an equation of the form

$$M = \frac{M_0[1 - \exp(-\mathrm{TR}/T_1)]}{[1 - \cos(\alpha)\exp(-\mathrm{TR}/T_1)]}. \qquad [12]$$

This allowed estimation of T_1, which was found to range between 0.10 and 0.75 s.

The errors in T_1 measurement for the snapshot-FLASH sequence were evaluated by comparing the values estimated using Eqs. [6], [7], and [9] to those obtained using the saturation-recovery method. One of the solutions of Gd-DTPA had a T_1 similar to that of myocardium (0.75 s); this vial mimicked the precontrast T_1 of myocardium and was used to assess the accuracy of Eq. [10] in predicting the inversion time to null a particular T_1. All snapshot-FLASH measurements were repeated four times, to ascertain the standard deviation of the T_1 measurement.

First, TR_0 was varied as a multiple of the myocardial-equivalent T_1 (T_1pre = 0.75 s), from 0.5 × T_1pre through 1 × T_1pre, to greater than 5 × T_1pre, in order to simulate different R–R intervals and multiples of the R–R interval. For each TR_0, the inversion time was such that the myocardium equivalent solution should have remained nulled if Eq. [10] proved to be accurate. The other acquisition parameters for the snapshot-FLASH sequence were α = 8°; TR = 4.7 ms; TE = 2 ms; FOV = 300 mm; 64 × 64 data matrix; 1 slice of 15 mm thickness. Eleven consecutive images at each TR_0 were obtained to ensure that the magnetization reached a steady state from one image to the next; the signal intensity used in the analysis below was always measured from the final image. In addition, a single image was acquired after full relaxation and without an inversion prepulse, the ''M_0'' scan.

Next, the effect of changing the flip angle of the α pulses on the accuracy of T_1 measurement was investigated. Scans were performed using flip angles of 1°, 8°, and 15°, for TR_0 corresponding to the myocardial T_1 (TR_0 = T_1pre = 0.75 s). Fifteen degrees is the largest flip angle allowed with this sequence on our MRI scanner.

The snapshot-FLASH sequence was then applied to measuring *in vivo* myocardial T_1. Fourteen patients admitted to our hospital with acute myocardial infarction were scanned within 2–4 days of this ischaemic event. These patients were also assessed using thallium-201 single photon emission computed tomography (SPECT).

Short axis images through the left ventricle were obtained using a three-slice snapshot-FLASH sequence, the slices being positioned above, through, and below the papillary muscle. The acquisition parameters were α = 8°; TR = 4.7 ms; TE = 2 ms; TI = 300 ms; FOV = 250 mm; 64 × 64 data matrix; 10 mm thick slices. Acquisition was cardiac gated so that the mid-line of *k* space was acquired in mid-diastole, and the inversion time was chosen to null the signal from myocardium precontrast.

First, an M_0 image was acquired for each slice by turning off the inversion pulse. Next, the heart was imaged continuously during the injection of 0.05 mmol kg^{-1} gadobenate dimeglumine (Gd-BOPTA) contrast agent (Bracco SpA, Milan, Italy). Images were acquired at a rate of one image every two heartbeats. The time interval between each of the snapshot-FLASH measurements was recorded for each patient.

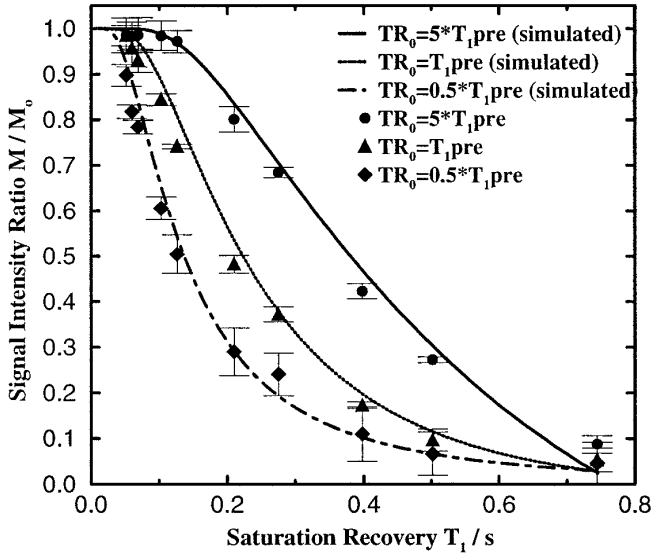

FIG. 6. Normalized signal-intensity response for the snapshot-FLASH pulse sequence for three values of TR_0, flip angle = 8°. Simulated and mean measured data (±2 standard deviations) are shown. The experimental data were measured from a phantom consisting of vials containing known concentrations of Gd-DTPA in aqueous solution. For each value of TR_0, the inversion time was adjusted so that the signal from the vial with T_1 = 750 ms was nulled.

Twenty images were obtained at each of the three myocardial levels, but only results from above the papillary muscle are presented here. On each image, including the M_0 images, the left ventricular myocardium was divided radially and evenly into 10 regions of interest (ROIs), and the mean signal intensity was found for each ROI. The R_1 (= $1/T_1$) for each sector of the myocardium was calculated twice, first with the simplified equation, Eq. [9], then using the full analysis of Eq. [6].

The differences caused by using the simplified versus the full analysis were then assessed in 10 ROIs per patient. Some ROIs were in areas that appeared to have normal uptake of thallium-201, while others were in areas with an abnormal (reduced) uptake. The results shown are averages of all the representative ROIs for the patients at all times during the contrast injection.

RESULTS

The magnetization values were sampled using ROIs encompassing approximately 20 pixels for both the phantom and cardiac studies. A correction for background noise in

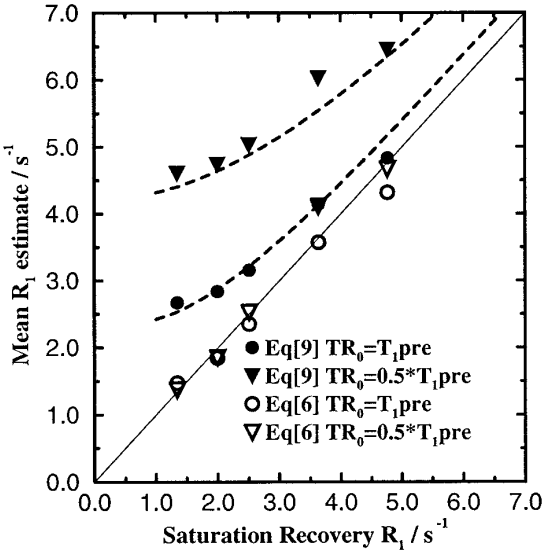

FIG. 7. Mean estimation of R_1 for three values of TR_0 using the simplified analysis of Eq. [9], and the full analysis of Eq. [6], for $TR_0 = T_1$pre and $TR_0 = 0.5T_1$pre. These are the same experimental data as shown in Fig. 6, presented to show the errors that occur in R_1 estimation when using the simple analysis. The dashed lines represent the theoretical R_1 estimates that would be expected when using Eq. [9] to analyze data with short TR_0 and $\alpha = 8°$.

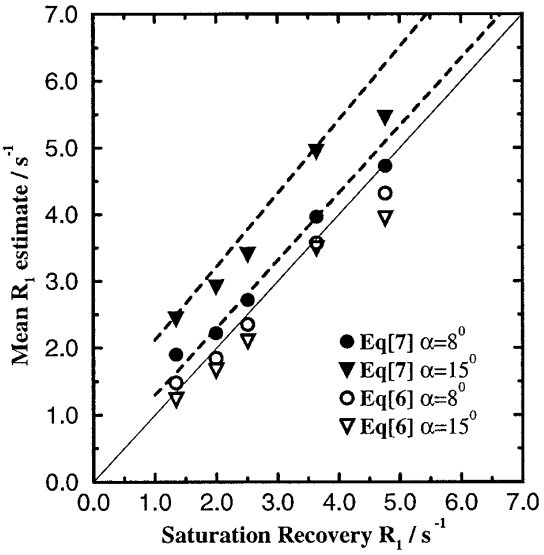

FIG. 8. Estimation of R_1 using the snapshot-FLASH pulse sequence for flip angles of 8° and 15° and $TR_0 = T_1$myo; other sequence parameters are given in the text. The phantom consisting of vials containing water doped with Gd-DTPA was again used in this experiment. R_1 was estimated using the low-flip-angle approximation of Eq. [7], and using the full analysis of Eq. [6]. The error introduced by the low-flip-angle approximation is relatively small until the flip angle exceeds about 8°. The dashed lines represent the theoretical R_1 estimates that would be expected when using Eq. [7] to fit to data where the flip angle cannot be considered small.

these magnitude images was performed using the method described by Henkelman (*18*), the magnitude of the noise having been measured in a region of the image outside the sample.

Figure 6 shows ratios of magnetization measured using the snapshot-FLASH sequence in steady state to that without the inversion prepulse. The magnetization ratio for three values of TR_0 ($5 \times T_1$pre, $1 \times T_1$pre, and $0.5 \times T_1$pre) overlays the theoretical curves calculated using Eq. [6]. The ratios shown represent the mean of the four measurements, and the error bars represent ± 2 standard deviations. Note that nulling of the myocardium-equivalent solution is maintained throughout the changes in TR_0 by adjustment of the inversion time. TI_{eff} was reduced from 519 ms for the longest TR_0 down to 165 ms for the shortest TR_0.

The estimates of T_1 using Eq. [6] or Eq. [7] were made using an iterative search scheme. Either Eq. [6] or Eq. [7] was used to predict the signal-intensity ratio (magnetization in steady state to magnetization when measured without an inversion pulse), and the value of T_1 in these equations was systematically searched in order to find that which gave the measured intensity ratio. The flip angle in Eq. [6] was fixed to the value calibrated by the scanner.

Figure 7 summarizes the errors that are introduced into the estimation of R_1 by using Eq. [9], when TR_0 is reduced. The mean and standard deviation of the R_1 values were calculated using Eq. [9] and the full Eq. [6]. These values are plotted against the R_1 measured using the saturation-recovery sequence, for the values of TR_0: $5 \times T_1$pre, $1 \times T_1$pre, and $0.5 \times T_1$pre ($\alpha = 8°$). Also shown are theoretical curves representing the expected behavior of the magnetization using Eq. [6], but analyzed using Eq. [9]. When $TR_0 > 5 \times T_1$pre, both methods yielded essentially the same result and were in agreement with the saturation-recovery measurement of T_1; these data are not plotted. However, as TR_0 is reduced, the use of Eq. [9] introduces considerable error at the shorter R_1 values. The TR_0 reduction from $1 \times T_1$pre to $0.5 \times T_1$pre also increased the standard deviation of the R_1 for Eq. [6] from 0.17 to 0.69 s^{-1} and for Eq. [9] from 0.11 to 0.40 s^{-1} respectively. This was due to the reduced signal-to-noise ratio at the lower values of TR_0.

The accuracy of T_1 measurement at flip angles of 1°, 8°, and 15° was calculated using Eq. [7], which does not allow

TABLE 1
Standard Deviation of R_1 for Each Flip Angle Using the Simple and Full Analysis

	Flip Angle of α pulses		
Equation used	1°	8°	15°
Simple analysis Eq. [7]	0.73 s^{-1}	0.15 s^{-1}	0.22 s^{-1}
Full analysis Eq. [6]	0.69 s^{-1}	0.17 s^{-1}	0.2 s^{-1}

TABLE 2
Calculated Relaxation Rates when Using the Simplified Analysis of Eq. [9] Compared to the Full Analysis of Eq. [6] for Human Myocardium during the Arterial Injection of Gd-BOPTA

	Slow heart rate (<80 bpm)			Fast heart rate (>80 bpm)		
	Using Eq. [6]	Using Eq. [9]	Percentage difference	Using Eq. [6]	Using Eq. [9]	Percentage difference
Mean R_1 in normal myocardium	2.16 s^{-1}	2.32 s^{-1}	7.7%	2.39 s^{-1}	2.67 s^{-1}	11.9%
Mean R_1 in infarcted myocardium	2.04 s^{-1}	2.24 s^{-1}	9.6%	1.63 s^{-1}	2.05 s^{-1}	25.3%

Note. The error introduced by the simplified analysis is higher for this cardiac-gated study at higher heart rates and for infarcted tissue.

for the effect of larger flip angles, and also using Eq. [6]. In Fig. 8, a systematic error in R_1 can be seen at the highest flip angle, which is corrected by the use of Eq. [6]. The data for a flip angle of 1° showed the most unbiased estimate of R_1 compared to the saturation-recovery method, but for clarity are not plotted. However, because of the poor signal-to-noise ratio, this flip angle also showed the highest mean standard deviations for both Eq. [7] and Eq. [6], compared to the higher flip angles; the standard deviations are shown in Table 1.

The patient data were divided (arbitrarily) into two groups: those with a slow heart rate (less than 80 beats per minute [bpm]) (8 patients) and those with a fast heart rate (>80 bpm) (6 patients). Table 2 summarizes the errors that occur when the simplified analysis (Eq. [9]) is used to estimate R_1. The mean difference in R_1 between the two methods of analysis was 10.5% which was statistically significant ($p < 0.001$; Student's t test for paired data). The difference was much greater for those patients with a high heart rate because of increased magnetization saturation caused by the shorter sequence repetition time. Also, because of the reduced R_1 in regions of infarction, the error was also greater in these areas (Table 2).

DISCUSSION

We have looked at the effects of flip angle of the α pulses and of reduction in the overall sequence repetition time on the calculation of T_1 from snapshot-FLASH images. If these factors are ignored, there will be a systematic underestimation of T_1. The application of Eq. [6] allows for the saturation of the magnetization and leads to accurate T_1 estimation even at short TR_0, and practical flip angles.

This work has implications for dynamic studies where a rapid series of snapshot-FLASH images is acquired, such as fast cardiac-gated T_1 imaging during the passage of a bolus of contrast agent (*19*). If T_1 can be measured accurately then it may be possible, through the change in concentration of a contrast agent, to quantify myocardial perfusion (*17, 20*).

It can be seen from Fig. 3 that deviations in the flip angle do not have a major impact on the computed T_1 for moderate changes of flip angle. It is therefore expected that if the flip angle varies throughout the slice, as can be the case for the short RF pulses used in snapshot-FLASH, then this should not affect the computed T_1 greatly. We have shown that, although the flip angle of the α pulses contributes to inaccuracy, the largest effect is due to the reduction in overall sequence repetition time.

The use of short overall sequence repetition times has consequences for the range of T_1 values that can be measured accurately. As can be seen from Fig. 2, a common problem is the inaccuracy in T_1 estimation at low values of T_1: magnetization recovers very quickly with almost complete relaxation after the inversion pulse and very little signal decrease up to quite large values of T_1. As TR_0 is reduced, the change in signal intensity with T_1 becomes considerably greater at these low T_1 values. However, this is at the expense of the very flat response around the null point. This latter point necessitates using a scheme for the correction of noise (*18*) if accurate T_1 measurement is to be maintained for T_1 values around the null point.

The accurate measurement of T_1 *in vivo* has many other problems not encountered in phantoms. We performed our phantom measurements on a system with monoexponential T_1 and applied this model to *in vivo* measurement. However, *in vivo* there may be multiple T_1 values as tissue water is compartmentalized (*21*). The measurement of multiexponential T_1 relaxation requires that several images are acquired at different points in the T_1 relaxation curve (*8*). If this is done with cardiac gating, then several cardiac cycles are needed. For dynamic imaging with good time resolution, this is not practical.

Note that using the full analysis of Eq. [6] has much greater impact on the R_1 estimates for the poorly perfused or infarcted tissue, since this has relatively long relaxation times.

CONCLUSIONS

We have shown that a simplistic analysis of the snapshot-FLASH sequence can lead to significant errors in T_1 mea-

surement if either the overall sequence repetition time is reduced to improve temporal resolution or large-flip-angle readout α pulses are used. We present a fuller analysis that takes into account both of these effects and removes their distorting influences. An additional benefit of using a shortened overall sequence repetition time is that the accuracy of the estimated T_1 should be improved at low T_1 values. However, this is at the expense of sensitivity at higher T_1.

The improved accuracy of monoexponential T_1 estimates has implications not only for perfusion studies of the heart, but for any system where rapid T_1 measurements are required.

ACKNOWLEDGMENTS

The authors express their thanks to Bracco SpA, Milan, Italy, who funded this work, and Siemens A.G. Medical Technology, Erlangen, Germany, for technical assistance that made this study possible. We are also grateful to the reviewers of the original manuscript for their detailed and helpful suggestions.

REFERENCES

1. R. Damadian, *Science* **171,** 1151 (1971).
2. P. A. Bottomley, C. J. Hardy, R. E. Argersinger, and G. Allen-Moore, *Med. Phys.* **14,** 1 (1987).
3. G. Johnson, I. E. Ormerod, D. Barnes, P. S. Tofts, and D. McManus, *Br. J. Radiol.* **60,** 142 (1987).
4. M. E. Masterson, R. McGary, K. Schmitt, and J. A. Koucher, *Med. Phys.* **16,** 225 (1989).
5. G. Brix, L. R. Schad, M. Deimling, and W. J. Lorenz, *Magn. Reson. Imaging* **8,** 351 (1990).
6. D. C. Look and D. R. Locker, *Rev. Sci. Instrum.* **41,** 250 (1970).
7. R. Graumann, M. Deimling, T. Heilmann, and A. Oppelt, Abstracts of the Society of Magnetic Resonance in Medicine, 4th Annual Meeting, p. 922, 1986.
8. A. P. Crawley and R. M. Henkelman, *Magn. Reson. Med.* **7,** 23 (1988).
9. I. Kay and R. M. Henkelman, *Magn. Reson. Imaging* **22,** 414 (1991).
10. P. A. Gowland and M. O. Leach, *Magn. Reson. Med.* **26,** 79 (1992).
11. Y. T. Zhang, H. N. Yeung, P. L. Carson, and J. H. Ellis, *Magn. Reson. Med.* **25,** 337 (1992).
12. R. Graumann, H. Barfuß, D. Hentschel, and A. Oppelt, *Electromedica* **55,** 67 (1987).
13. A. Haase, *Magn. Reson. Med.* **13,** 77 (1990).
14. R. Deichmann and A. Haase, *J. Magn. Reson.* **96,** 608 (1992).
15. S. Bluml, L. R. Schad, B. Stepanow, and W. J. Lorenz, *Magn. Reson. Med.* **30,** 289 (1993).
16. E. Rostrup, H. B. W. Larsson, T. Fritz-Hansen, P. Ring, and O. Henriksen, ''Book of Abstracts: Proceedings of the Society of Magnetic Resonance, and European Society for Magnetic Resonance in Medicine and Biology,'' p. 1062, 1995.
17. H. B. W. Larsson, M. Stubgaard, L. Søndergaard, and O. Henriksen, *J. Magn. Reson. Imaging* **4,** 433 (1994).
18. R. M. Henkelman, *Med. Phys.* **12,** 232 (1985).
19. N. Wilke, M. Jerosch-Herold, A. E. Stillman, K. Kroll, N. Tsekos, H. Merkle, T. Parrish, X. Hu, and Y. Wang, *Magn. Reson. Q.* **10,** 249 (1994).
20. L. Diesbourg, F. S. Prato, G. Wisenberg, D. J. Drost, T. P. Marshall, S. E. Carrol, and B. O'Neil, *Magn. Reson. Med.* **23,** 239 (1992).
21. D. Burstein, E. Taratuta, and W. J. Manning, *Magn. Reson. Med.* **20,** 299 (1991).